Quantitative Cerebral Blood Flow with PET in the 1980s: Going with the Flow

Richard E. Carson

Yale University, New Haven, Connecticut

Nuclear medicine in general and PET imaging in particular have long provided the opportunity for quantitative measurements of human physiology in vivo. Practical methodology for these measurements came to pass in the late 1970s and early 1980s as PET scanners provided quantitative images of radioactivity in humans after injection of radiopharmaceuticals. Furthermore, studies on the human brain became a focus because image quality for the brain was far superior to that for other parts of the body, for reasons such as the lower attenuation in the head. An obvious target for quantification was cerebral blood flow (CBF), using the elegantly simple flow agent ^{15}O-water. After intravenous injection, water arrives rapidly in the brain and is extracted with high efficiency, so that the initial uptake is nearly proportional to blood flow.

Received Jun. 22, 2020; revision accepted Jun. 26, 2020.
For correspondence or reprints contact: Richard E. Carson, Yale University, P.O. Box 208048, New Haven, CT 06520.
E-mail: richard.carson@yale.edu

DOI: 10.2967/jnumed.120.252130

In the 1980s, several groups were working on methods for quantification of blood flow with ^{15}O-water. The Washington University group developed elegant quantification methods, presented in seminal papers by Herscovitch et al. and Raichle et al. in 1983 (*1*,*2*). The methodology was challenging, involving producing an isotope with a 2-min half-life, rapidly producing labeled water in injectable form, delivering a bolus injection with more than 925 MBq (25 mCi) of activity, rapidly collecting arterial samples to define the blood time–activity curve, and, of course, acquiring and reconstructing PET images. These were not experiments to be undertaken by the faint of heart.

The 1983 papers of Herscovitch, Raichle, and their colleagues exemplified the ideal approach for development of quantitative imaging assays with PET. First, the authors based their studies on classic tracer methods and kinetic modeling techniques, in which they used equations to explain the relationship between the tissue radioactivity data and the underlying physiologic parameter of interest, that is, CBF. They used nonhuman primate studies to validate the PET measures against established, nontomographic flow approaches. Further, they found ways to simplify the approach

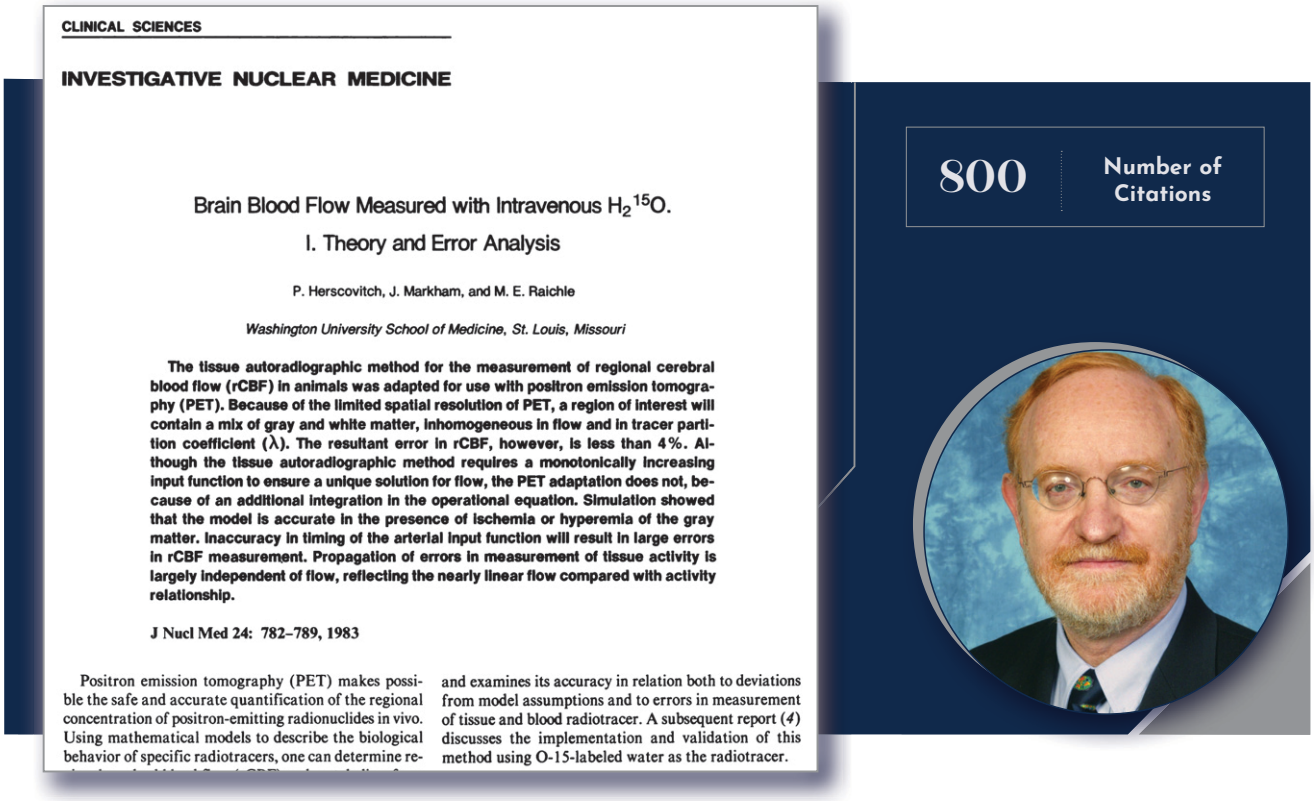
CLINICAL SCIENCES

INVESTIGATIVE NUCLEAR MEDICINE

Brain Blood Flow Measured with Intravenous $H_2{}^{15}O$.
I. Theory and Error Analysis

P. Herscovitch, J. Markham, and M. E. Raichle

Washington University School of Medicine, St. Louis, Missouri

The tissue autoradiographic method for the measurement of regional cerebral blood flow (rCBF) in animals was adapted for use with positron emission tomography (PET). Because of the limited spatial resolution of PET, a region of interest will contain a mix of gray and white matter, inhomogeneous in flow and in tracer partition coefficient (λ). The resultant error in rCBF, however, is less than 4%. Although the tissue autoradiographic method requires a monotonically increasing input function to ensure a unique solution for flow, the PET adaptation does not, because of an additional integration in the operational equation. Simulation showed that the model is accurate in the presence of ischemia or hyperemia of the gray matter. Inaccuracy in timing of the arterial input function will result in large errors in rCBF measurement. Propagation of errors in measurement of tissue activity is largely independent of flow, reflecting the nearly linear flow compared with activity relationship.

J Nucl Med 24: 782–789, 1983

Positron emission tomography (PET) makes possible the safe and accurate quantification of the regional concentration of positron-emitting radionuclides in vivo. Using mathematical models to describe the biological behavior of specific radiotracers, one can determine re- and examines its accuracy in relation both to deviations from model assumptions and to errors in measurement of tissue and blood radiotracer. A subsequent report (*4*) discusses the implementation and validation of this method using O-15-labeled water as the radiotracer.

800 Number of Citations

to make it practical, given the acquisition limitations of the systems of that era. The kinetic model was reformulated to allow measurement of one image with one scan (i.e., one equation and one unknown). To do this, the authors added a physiologically reasonable constraint for the partition coefficient of water in the brain. Finally, the authors developed a simple implementation of the model to allow the creation of CBF images from the reconstructed radioactivity images that did not overly tax the capabilities of the minicomputers of the day.

Other investigators of the era used different analytic approaches, still applying bolus injections of ^{15}O-water and rapid arterial sampling (*3,4*). These techniques extended the methodology, finding novel ways to use the dynamic nature of tracer influx and efflux, even though dynamic scans were not readily available. Today, things are different, and they are also exactly the same. Yes, our systems are much more powerful, with far greater sensitivity, resolution, accuracy, and precision. The image quality we see today was unimaginable in 1983. But practically, this simply comes down to having more counts and more pixels (and, fortunately, much faster computers). The fundamentals of physiology and pharmacology have not changed. We continue to apply similar tools and methods that follow the approaches exemplified in these papers. Using specific radiopharmaceuticals, we develop kinetic modeling methods and experimental designs to quantify brain proteins, receptors, enzymes, and transporters (*5*). We validate the methodology with animal studies and human drug occupancy experiments. Then, we find ways to simplify the analysis approaches, such as Patlak and Logan graphical analysis methods. Further, we can use our understanding of the tracer's characteristics to produce more patient-friendly approaches by using SUVs (e.g., for ^{18}F-FDG) or SUV ratios (e.g., for amyloid or tau brain imaging). All of these approaches have been more commonly applied for brain imaging, in part because of better quantification accuracy in the brain (e.g., simpler, rigid head motion), as well as the blood–brain barrier that restricts entry of radiolabeled metabolites. However, there is recent growth in the development and application of patient-friendly quantitative physiologic methods for body imaging.

And what about the measurement of CBF with PET today; are we still going with the flow? With the advent of functional MRI (blood oxygenation level–dependent and arterial spin labeling), PET is seldom used in investigations of CBF (although it was extensively used to validate functional MRI methods). To my mind, the transfer of CBF studies from PET to MRI was one of the best things that could have happened to brain PET. Instead, we in nuclear medicine can focus on what we do best and what we can uniquely do, that is, develop and apply specific radiopharmaceuticals operating in picomolar quantities to measure virtually any aspect of human biology.

DISCLOSURE

No potential conflict of interest relevant to this article was reported.

REFERENCES

1. Herscovitch P, Markham J, Raichle ME. Brain blood flow measured with intravenous $H_2{}^{15}O$. I. Theory and error analysis. *J Nucl Med*. 1983;24:782–789.
2. Raichle ME, Martin WR, Herscovitch P, Mintun MA, Markham J. Brain blood flow measured with intravenous $H_2{}^{15}O$. II. Implementation and validation. *J Nucl Med*. 1983;24:790–798.
3. Huang SC, Carson RE, Phelps ME. Measurement of local blood flow and distribution volume with short-lived isotopes: a general input technique. *J Cereb Blood Flow Metab*. 1982;2:99–108.
4. Alpert NM, Eriksson L, Chang JY, et al. Strategy for the measurement of regional cerebral blood flow using short-lived tracers and emission tomography. *J Cereb Blood Flow Metab*. 1984;4:28–34.
5. Hooker JM, Carson RE. Human positron emission tomography neuroimaging. *Annu Rev Biomed Eng*. 2019;21:551–581.

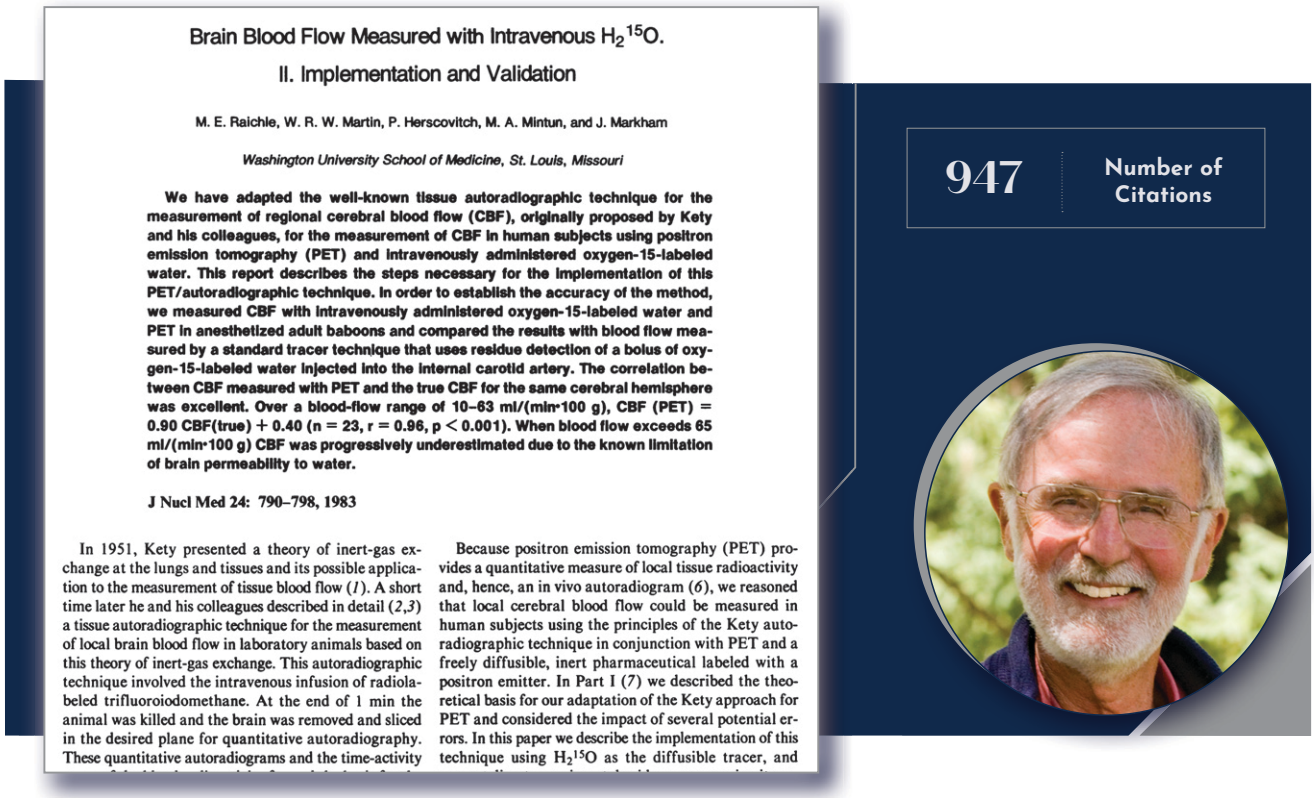

Brain Blood Flow Measured with Intravenous $H_2{}^{15}0$. I. Theory and Error Analysis

P. Herscovitch, J. Markham, and M. E. Raichle

Washington University School of Medicine, St. Louis, Missouri

The tissue autoradiographic method for the measurement of regional cerebral blood flow (rCBF) in animals was adapted for use with positron emission tomography (PET). Because of the limited spatial resolution of PET, a region of interest will contain a mix of gray and white matter, inhomogeneous in flow and in tracer partition coefficient (λ). The resultant error in rCBF, however, is less than 4%. Although the tissue autoradiographic method requires a monotonically increasing input function to ensure a unique solution for flow, the PET adaptation does not, because of an additional integration in the operational equation. Simulation showed that the model is accurate in the presence of ischemia or hyperemia of the gray matter. Inaccuracy in timing of the arterial input function will result in large errors in rCBF measurement. Propagation of errors in measurement of tissue activity is largely independent of flow, reflecting the nearly linear flow compared with activity relationship.

J Nucl Med 1983; 24:782–789
DOI: 10.2967/jnumed.120.252130a

Positron emission tomography (PET) makes possible the safe and accurate quantification of the regional concentration of positron-emitting radionuclides in vivo. Using mathematical models to describe the biological behavior of specific radiotracers, one can determine regional cerebral blood flow (rCBF) and metabolism from the radioactivity concentrations of blood and local tissue. The soundness of physiological measurements made with PET depends not only on accurate radiotracer quantification by the tomographic scanner, but also on the validity of assumptions inherent in the physiological model and the sensitivity of the model to errors in the measurements of tissue and blood radioactivity.

We have proposed that the tissue autoradiographic method for the measurement of rCBF in animals, originally developed by Kety and his colleagues (*1,2*) can be adapted for in vivo rCBF determination with PET (*3*). This report describes in detail such a PET adaptation and examines its accuracy in relation both to deviations from model assumptions and to errors in measurement of tissue and blood radiotracer. A subsequent report (*4*) discusses the implementation and validation of this method using O-15-labeled water as the radiotracer.

Received Dec. 21, 1982; revision accepted Apr. 28, 1983.
For reprints contact: M. E. Raichle, Washington University School of Medicine, 510 South Kingshighway, St. Louis, MO 63110.

THEORY

The tissue autoradiographic method for the measurement of rCBF, based on the principles of inert gas exchange between blood and tissues developed by Kety (*5*), has been widely used in laboratory animals (*1,6*). A freely diffusible, biologically inert radiotracer is infused intravenously for a brief time period, T, followed by decapitation of the animal. rCBF is obtained by numerically solving the following equation for f, the flow per unit weight of tissue:

$$\begin{aligned} C_i(T) &= f\int_0^T C_a(t)\exp[-f/\lambda(T-t)]dt \\ &= fC_a(T)^*\exp[-(f/\lambda)T], \end{aligned} \quad (1)$$

where $C_i(T)$ is the instantaneous local tissue radiotracer concentration (cps/unit weight) after an infusion time of T seconds, derived from a quantitative autoradiogram of a brain slice; $C_a(t)$ is the measured concentration of radiotracer in arterial blood as a function of time; and λ is the brain:blood equilibrium partition coefficient for the tracer. The asterisk denotes the operation of convolution. The derivation of Eq. (1) is based on a one-compartment model in which flow and λ are considered homogeneous in a region of interest. It is assumed that rCBF remains constant during the period of measurement.

Current PET scanners cannot measure the instantaneous tissue count rate, $C_i(T)$. A scan must be performed over many seconds, essentially summing the decay events occurring during the scan. One obtains an image of local counts collected during the scan, not of instantaneous count rate. Therefore, to adapt the tissue autoradiographic technique for in vivo studies with PET, we have modified the operational Eq. (1) of this model by an integration of the instantaneous count rate, $C_i(T)$, over the time of the scan, T_1 to T_2, as follows:

$$\begin{aligned} C &= \int_{T_1}^{T_2} C_i(T)dT \\ &= f\int_{T_1}^{T_2} C_a(T)^*\exp[-(f/\lambda)T]dT \end{aligned} \quad (2)$$

Here, C is the local number of counts per unit weight of tissue recorded by the tomograph from a region of brain during the scan. The arterial activity curve $C_a(t)$ is determined by frequent arterial blood sampling, and both the PET scan data and the blood curve are corrected for the decay of radiotracer that occurs following its intravenous injection. Once a value of λ is specified (see below), Eq. (2) can be solved numerically for flow for any specific region in the tomographic image. Alternatively, a look-up table calculated from Eq. (2) may be used to relate local tissue counts to rCBF (*7*).

Several potential sources of error have been identified for the tissue autoradiographic method, and their impact must be considered in this PET adaptation. These difficulties include inhomogeneity of tissue with respect to flow (*8*), uncertainty in the exact value of λ, the partition coefficient for the radiotracer (*8*), restrictions on the shape of the arterial concentration input function $C_a(t)$ (*9*), and uncertainty in the timing of $C_a(t)$ (*10*). The PET adaptation of the autoradiographic method might introduce further errors in flow measurement related to the limited spatial resolution of the scanner (*11*), to the performance of the model when applied to disease conditions, and to the impact of error in the measurement of local tissue radioactivity with the scanner. These potential sources of inaccuracy in the PET autoradiographic method, and a computer simulation to study their impact, will now be discussed.

METHODS OF ERROR ANALYSIS

Our approach to rCBF measurement with PET is based on a one-compartment model that assumes that the tissue in which the local radioactivity measurement is made is homogeneous with respect to flow and λ. However, because of the limited spatial resolution of PET—currently in the range of 1–1.5 cm (*12,13*)—a region of interest (ROI) will contain a mix of gray and white matter inhomogenous in both flow and λ. Thus an average λ must be selected for use in the operational equation, Eq. (2), and the resultant measured flow will reflect some nonlinear combination of the gray and white matter flows in the ROI.

A computer simulation was developed to study the effect of tissue inhomogeneity and other possible sources of error. The simulation is based on the following principles. A tissue ROI may be considered to contain varying fractions, w_g, and w_w, of gray and white matter respectively, where $w_g + w_w = 1$. One may specify the flow, f, and the known λ for gray or white matter, and an arbitrary arterial radiotracer time-activity curve, $C_a(t)$, and then apply Eq. (2) to calculate the tissue counts, C_g or C_w that would be obtained if the ROI consisted only of gray or white matter. The following relations are obtained for gray and white matter, respectively:

$$C_g = f_g \int_{T_1}^{T_2} C_a(T)^* \exp\left[-\left(f_g/\lambda_g\right)T\right]dT \quad (3)$$

$$C_w = f_w \int_{T_1}^{T_2} C_a(T)^* \exp\left[-\left(f_w/\lambda_w\right)T\right]dT \quad (4)$$

Then, for relative weights, w_g and w_w, of gray and white matter in the ROI, the regional tissue counts that would be obtained with a PET scan for these weights is

$$C = W_g C_g + W_w C_w. \quad (5)$$

This weighted count value, C, is then used in Eq. (2) along with the specified arterial time-activity curve and an average brain λ to calculate the "measured" flow. This is to be compared with the "true" flow in the ROI, that is the weighted sum of gray and white flows

$$f_{true} = W_g f_g + W_w f_w \quad (6)$$

Any difference between these two flow values reflects an error in rCBF measurement due to the specified degree of tissue inhomogeneity in the ROI.

In addition, this computer simulation can be used to investigate a wide variety of other possible sources of error in rCBF measurement. The shape of the arterial time-activity input function, $C_a(t)$, may affect the performance of the autoradiographic method. Ginsberg (*9*) has noted that the tissue autoradiographic method requires a monotonically increasing input function $C_a(t)$. Otherwise, a situation can develop in which different flows can give rise to the same local tissue radioactivity, and a unique flow result will not be obtained from Eq. (1). The effect of the input function in the PET adaptation of this method [Eq. (2)] is examined with the simulation by specifying various shapes for $C_a(t)$ in Eqs. (3) and (4).

Abnormal conditions, such as ischemia or neoplasm, can alter both the regional partition coefficient for the tracer and the degree of flow inhomogeneity. Performance of the PET autoradiographic method in such cases can be studied by specifying flows and/or λ in Eqs. (3) and (4) to simulate tissue disease, and then comparing the resultant "measured" flow with the true weighted regional flow.

Inaccuracy in the measurement of the tissue or arterial activity concentrations used in Eq. (2) will result in errors in flow calculation. Several inaccuracies are possible. In practice, the arterial blood curve is obtained by sampling from a peripheral artery. Since the distance from the heart to a peripheral artery (e.g., the femoral or radial) may be greater than the distance from heart to brain, the data points on the sample-derived curve can be delayed in time with respect to the true input function. In addition, difficulties in rapidly sampling arterial blood do lead to a less-than-perfect definition of the arterial input curve. Finally, error in measuring tissue activity with the PET system is propagated in the calculation of flow. The effect of these various measurement inaccuracies can be simulated. Equations (3) to (5) are used to calculate the true or expected tissue activity for a specified arterial input curve in a ROI. The calculated flow as affected by one of the above measurement errors is obtained by inserting the specific measurement error—either in tissue counts, C, or arterial activity, $C_a(t)$—in Eq. (2) before the flow is calculated, and then comparing this calculated flow with the true weighted regional flow from Eq. (6).

To facilitate these simulation studies, which involved manipulation of the arterial input function, $C_a(t)$ was approximated by the function $At \cdot t \cdot \exp(-t/t_p)$. This yields a rising, then falling curve with its peak value at time t_p. The arbitrary constant, A, can be adjusted such that the area under the input curve, which corresponds to the total decay-corrected activity injected, is held constant. A low value of t_p (e.g., 10 sec) results in an input waveform similar in shape to that obtained in practice with an intravenous bolus injection, whereas for long t_p, the rising part of the curve simulates an infusion input (see Fig. 3, upper left).

All of these simulation studies are based on a scan length of 40 sec ($T_2 - T_1$, Eq. 2), which is in keeping with the original measurement time of 1 min or less proposed by Kety and his colleagues (1,2,6,7). Unless otherwise specified, the value for average brain λ for water used in Eq. (2) is 0.95 ml $\cdot$ g^{-1}, and the arterial input is a bolus waveform reaching its peak at 10 sec.

RESULTS

The effect of tissue inhomogeneity in an ROI containing varying proportions of gray and white matter is shown in Fig. 1. The respective values of flow and λ used in Eqs. (3) and (4) were 80 ml $\cdot$ min^{-1} $\cdot$ hg^{-1} and 1.04 ml $\cdot$ g^{-1} in gray matter (*14*), and 20 ml $\cdot$ min^{-1} $\cdot$ hg^{-1} and 0.88 ml $\cdot$ g^{-1} in white matter (*14*). The

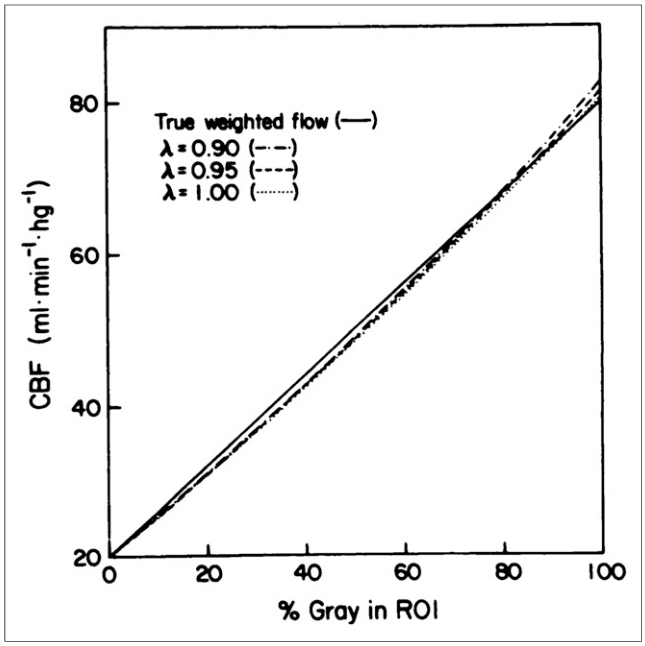

FIGURE 1. Calculated flow for regions of Interest with varying mixes of gray and white matter, for model with average partition coefficients of 0.90, 0.95, and 1.00 ml • g^{-1}. Solid line represents true weighted flow of the tissue mix. Arterial input function is bolus waveform reaching its maximum at 10 sec.

TABLE 1
Effect of the Shape of the Arterial Input Function on Calculated rCBF

% Gray in ROI	True flow in ROI	Calculated rCBF*			
		Step	10-sec peak	40-sec peak	60-sec peak
0	20	20.0	19.9	19.9	19.9
20	32	31.0	30.9	31.0	31.1
40	44	42.6	42.5	42.6	42.8
60	56	54.8	54.7	54.7	55.0
80	68	67.7	67.7	67.3	67.7
100	80	81.4	81.4	80.6	81.1

*Calculations made using a model λ of 0.95 ml • g^{-1} and a scan length of 40 sec. Flows are given in ml • min^{-1} • hg^{-1}. The input functions consisted (a) of a step function, and (b) of waveforms of shape $A \cdot t \cdot \exp(-t/t_p)$, with peak values reached at the times listed.

arterial input function had a bolus waveform reaching its peak at 10 sec. The calculated rCBF from the one-compartment PET autoradiographic model is very close to the true weighted flow over the whole range of possible tissue mixes, with the maximum error of −3.7% occurring in an ROI containing 70% white matter, using an average λ in Eq. 2 of 0.95 ml • g^{-1}. The calculated values for flow were relatively insensitive to the choice of the value for the average λ for the model, for example, 0.90, 0.95, or 1.00 ml • g^{-1}, as illustrated. In addition, the error in rCBF determination due to tissue inhomogeneity is affected little by the shape of the input function, as seen in Table 1.

The relationship between the tissue counts in an ROI and its true weighted flow was examined using Eqs. (3)–(6). In Fig. 2 this relationship is plotted for an 80% gray ROI, with gray flow varying from 10 to 100 ml • min^{-1} • hg^{-1}, and a ratio of gray-to-white flow of 4:1. Over the range of flow likely to be seen in humans, the number of local tissue counts is almost linearly related to flow. This has been found true regardless of the shape of the arterial input function, and of the weights and flows of gray and white matter in the ROI.

The effect of the shape of the arterial time-activity input curve on the solution of the original autoradiographic equation [Eq. (1)] for flow is illustrated in Fig. 3. Two inputs were used, a bolus input and a slowly changing infusion (Fig. 3, upper left). As seen in Fig. 3, upper right, for certain infusion times, a bolus input can give rise to the same tissue activity in regions that have different flows. The infusion times at which these multiple solutions occur depend upon the shape of the input function. With a bolus input reaching its peak in 10 sec, the first such time is at 84 sec, while a faster-rising bolus peaking in 5 sec leads to multiple solutions appearing earlier, at 71 sec. Thus, there is a potential for multiple solutions in the calculation of flow from a given tissue activity with the tissue autoradiographic method. This problem does not arise with a slowly changing infusion input. However, since the PET autoradiographic approach, as embodied in Eq. (2), involves an integration of tissue activity over time, this problem of multiple solutions with a bolus input does not arise over the equivalent time period (Fig. 3, lower left); in fact, the curves in tissue counts as a function of time continue to remain separated at 140 sec.

The effects of simulated abnormal tissue on rCBF determination are shown in Figs. 4 and 5. Cerebral ischemia or hyperemia was modeled by using as values for pure gray-matter flow 40, 60, 80, and 100 ml • min^{-1} • hg^{-1} in the calculation of regional gray-matter counts with Eq. (3). As seen in Fig. 4, the largest errors occur with the highest gray flow, with the maximum error being −6% in a 30% gray ROI. As gray flow decreases, the error in calculated flow decreases as well, since the inhomogeneity in the ROI with respect to flow is less. The ability of the PET autoradiographic method to quantify incremental changes in rCBF accurately is illustrated in Table 2. The changes in flow that would

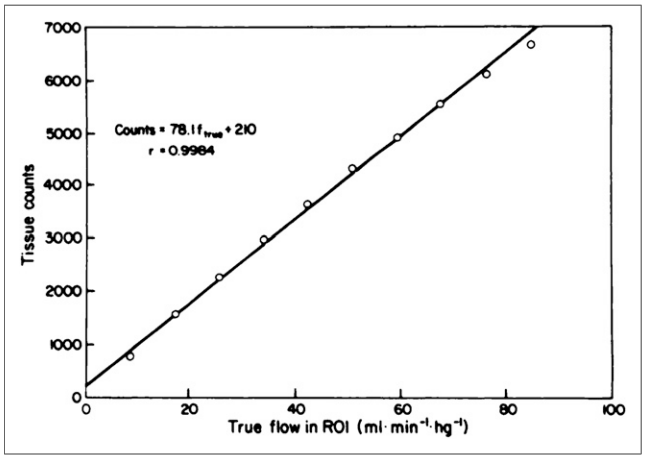

FIGURE 2. Relationship between true weighted flow and tissue counts in ROI that is 80% gray matter (see text).

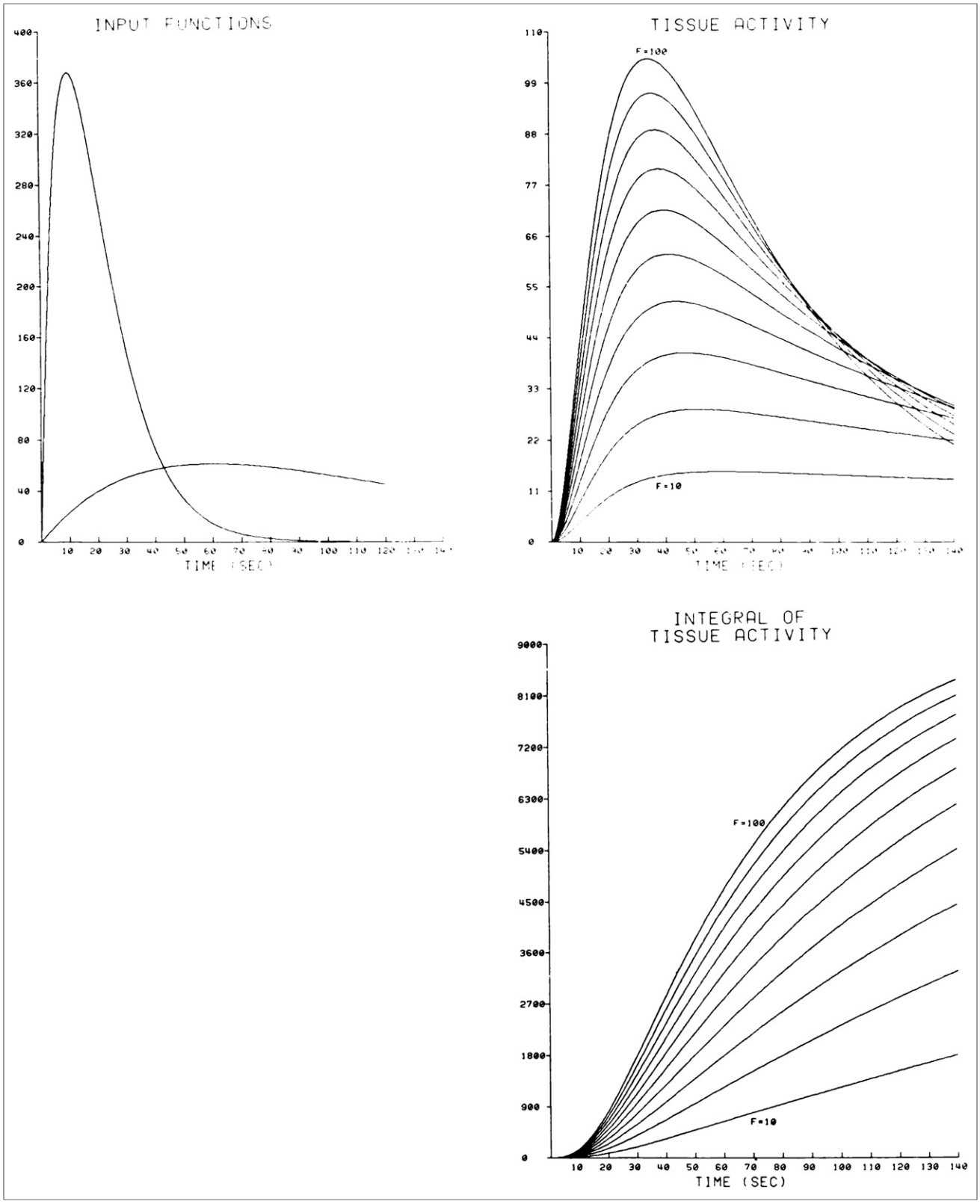

FIGURE 3. Effect of shape of arterial input function on uniqueness of solution for flow. Upper left: Illustration of arterial input functions used, of form $A \cdot t \cdot \exp(-t/t_p)$: a bolus type of waveform peaking at 10 sec, and slowly changing input whose rising part simulates infusion. Upper right: Tissue activity as function of time, with bolus input for tissue autoradiographic method. Activity curves are plotted for flows ranging from 10 to 100 ml $\cdot$ $min^{-1} \cdot hg^{-1}$. Below: Integrals of tissue activity for bolus input, as used in PET autoradiographic method, showing no possibility of multiple solutions for flow over time period indicated.

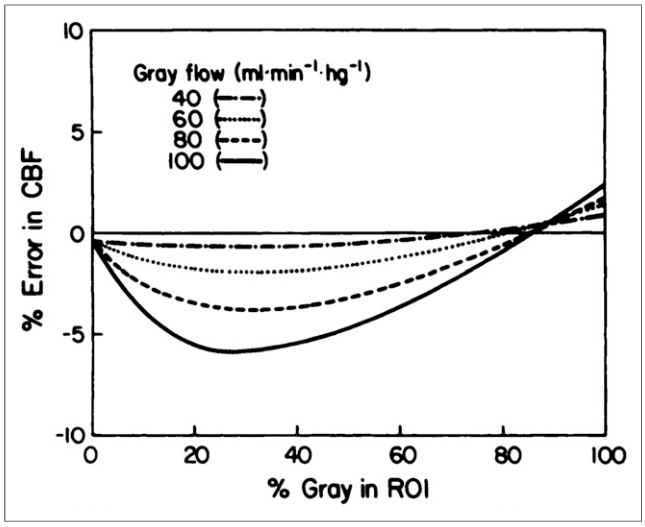

FIGURE 4. Percentage errors in calculated rCBF with various gray-matter flows simulating hyperemia (100 ml • min^{-1} • hg^{-1}) or ischemia (60 and 40 ml • min^{-1} • hg^{-1}), for varying gray: white mixes. White-matter flow is 20 ml • min^{-1} • hg^{-1}.

be measured with incremental changes in gray-matter flow of 20 ml • min^{-1} • h^{-1} are listed for various gray:white tissue mixes. These measured changes closely reflect the true weighted flow change in the ROI.

To simulate abnormal tissue such as a brain tumor in which λ may vary widely, flows were calculated for an ROI containing varying proportions of white matter and tissue, with abnormal λs of 0.90 and 1.05 ml • g^{-1}. The calculated flows that would be obtained in practice are very close to the true weighted regional flows, with the errors shown in Fig. 5. This is not surprising, given the relative insensitivity of the model to the value of average λ used in the operational Eq. (*2*), as noted above.

Inaccuracy in the timing of the arterial activity curve can cause large errors in rCBF measurement, as shown in Fig. 6. A moderate 2-sec delay in the sampled arterial activity curve with respect to the true arterial brain input causes a 4–10% over estimation of rCBF with a bolus input, while with a larger 5-sec delay, errors of up to +24% are obtained. Of note, for the same degree of delay,

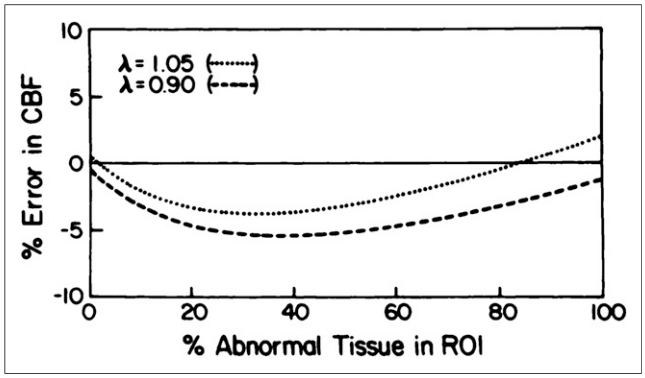

FIGURE 5. Percentage errors in calculated rCBF for ROI containing white matter with flow of 20 ml • min^{-1} • hg^{-1} and $\lambda_w = 0.88$ ml • g^{-1} and varying proportions of abnormal tissue, with flow of 80 ml • min^{-1} • hg^{-1} and with partition coefficients of 0.90 and 1.05 ml • g^{-1}.

TABLE 2
Measured Changes in rCBF With Incremental Changes in Gray Matter Flow of 20 ml • min^{-1} • hg^{-1}

% Gray in ROI	True change in rCBF in ROI	Measured changes in rCBF* for indicated changes in gray flow			
		100-80	80-60	60-40	40-20
100	20	21.0	20.6	20.5	20.2
90	18	18.2	17.9	18.2	18.1
80	16	15.4	15.7	15.9	16.0
70	14	13.1	13.3	13.7	14.0
60	12	10.8	11.2	11.6	11.9

*Calculations made using the same simulated conditions as in Table 1. White matter flow is 20 ml • min^{-1} • hg^{-1}.

larger errors are obtained with a slowly changing infusion input than with a bolus input. The effect of the frequency of sampling of the arterial activity curve, $C_a(t)$, on calculated flow was studied. In practice, discrete arterial samples are rapidly drawn at an interval of about every 5 sec. We compared calculated blood flow for this 5-sec and for a rapid 1-sec sampling frequency, using the bolus input function in Fig. 3, (upper left), in ROI with varying mixes of gray and white matter. The flows calculated from the less frequently sampled input differed no more than 3.6% from those calculated using the rapidly sampled input.

The effect of error in the measurement of regional tissue activity with PET on the resultant calculated rCBF is shown in Fig.

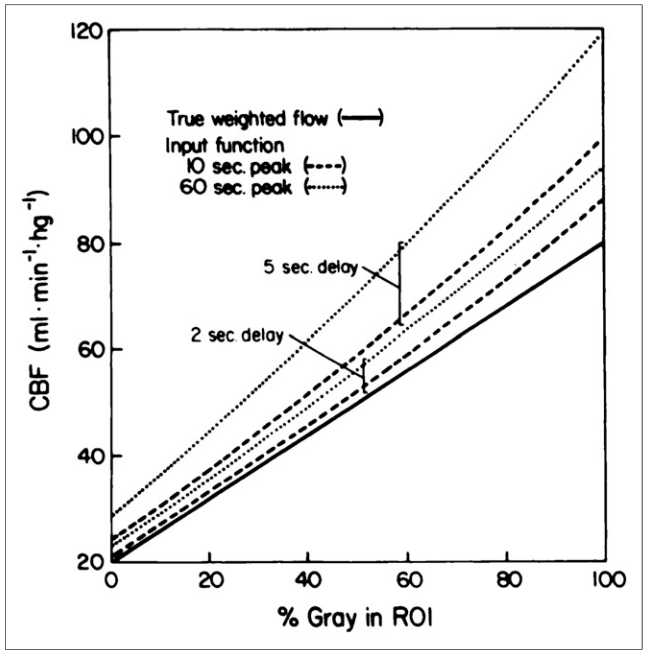

FIGURE 6. Effect of delay between curve for peripheral arterial samples and actual arterial input to brain. Resultant calculated flows are shown for 2-sec and 5-sec delays, for bolus input (10-sec peak) and infusion (60-sec peak).

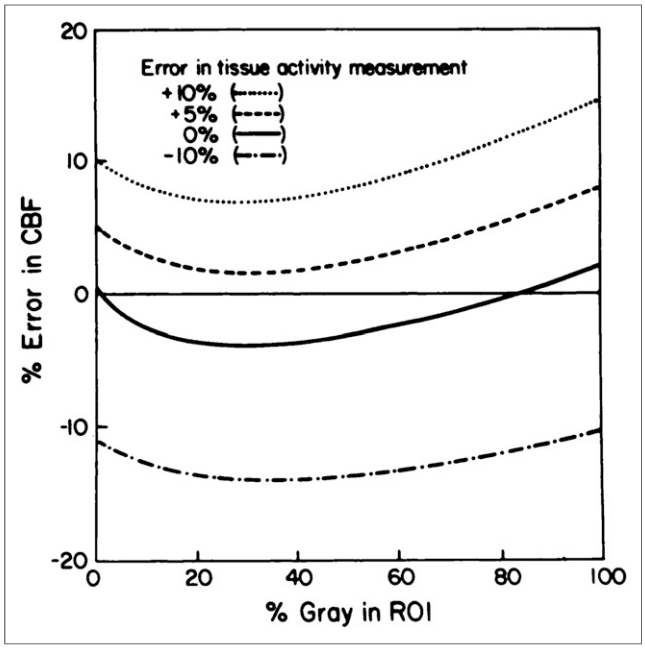

FIGURE 7. Effects of error in measurement of regional tissue activity on error in calculated flow.

7. The percent error in activity measurement is propagated as an approximately equivalent percent error in rCBF. In addition, the propagation of error in tissue activity measurement is essentially independent of flow rate.

DISCUSSION

The ability to measure cerebral blood flow is critical for an understanding of the pathophysiology of cerebrovascular and other neurological disorders. PET makes possible, for the first time, the safe and accurate in vivo quantification of rCBF in man. However, for reliable rCBF quantification with PET, the strengths and limitations of the physiological model used to calculate flow from blood and local tissue radiotracer measurements must be understood.

Although the tissue autoradiographic method, as well as its PET adaptation, is based on a one-compartment model, which assumes regional tissue homogeneity, the limited spatial resolution of PET will result in an ROI containing a mix of gray and white matter that is heterogeneous in both flow and λ. However, this study demonstrates that the rCBF measured in such a region will be very close to the true weighted gray and white flows in the region. Eklof (*8*) has demonstrated that the tissue autoradiographic method accurately reflects the true weighted flow in a gray-matter region that is heterogeneous in flow. Ginsberg et al. (*15*) used an autoradiographic strategy with an external probe system to measure global cerebral blood flow in the rat. Their model predicted reliable estimates of rCBF in simulated gray:white mixtures heterogeneous only in flow provided the white component was less than 25%. The analysis of our PET autoradiographic approach indicates that the rCBF measured in an ROI that is heterogeneous in both flow and λ will be within 4% of the true weighted flow regardless of the gray:white proportion.

The finding that rCBF and local tissue radioactivity are almost linearly related in the flow range likely to be encountered in human studies is of practical importance. Firstly, the image of tissue counts will linearly reflect relative differences in flow in different regions of the brain during the scan. Thus, for certain applications, such as functional mapping of the brain, where only relative changes in rCBF are sought, arterial blood sampling might not be required. Secondly, as seen in Table 2, the technique will accurately reflect changes in regional gray-matter flow in a linear fashion, although the change will be lessened by a factor equal to the fraction of gray matter in an ROI. Finally, the propagation of error in tissue radioactivity measurement in the calculation of flow will be approximately linear (see below).

The calculated blood flow was shown to be quite insensitive to the choice of average λ used in the PET operational equation. Eklof (*8*) reported a similar behavior for the tissue autoradiographic method with infusion times less than 60 sec and flows less than 100 ml • min^{-1} • hg^{-1}. This is a very useful property, since it is not, possible in general to use a λ weighted to the gray:white proportions in the ROI, as these proportions are not known in practice. In addition, although the λ in abnormal tissue, such as tumor, will generally be unknown, the routine use of an average λ results in little error. Thus, although it is based on a one-compartment model, the PET autoradiographic method will accurately quantify rCBF in inhomogeneous regions of tissue in both normal brain and in conditions that may change regional flow or λ.

The finding that a bolus input may be used in the PET method without the risk of multiple solutions for flow (as occurs in the tissue autoradiographic method) has important practical implications. Our PET method has been implemented using as the diffusible tracer water labeled with O-15, which has a 123-sec half-life. Thus, the use of a slow infusion of radiotracer during the length of the scan would result in considerable decay of the tracer during its infusion, with less activity being delivered to the brain than is desirable for reliable PET images.

It is important to understand the effects of inaccuracy in tissue and arterial activity measurements on the calculation of rCBF, and then to minimize the impact of these inaccuracies if possible. A mismatch in timing between the sampled peripheral arterial activity curve and the arterial input to the brain was shown to cause large errors in the calculated rCBF. This finding provides a motive for strategies to correct for these timing errors. One approach that has been implemented is to measure the difference in arrival times of the radiotracer bolus between the brain and the peripheral sampling site. This time difference is used to shift the peripheral-artery activity curve appropriately in time before using it for rCBF calculation. Relatively infrequent sampling of the arterial blood curve, e.g., every 5 sec, introduced rather small errors in rCBF. However, these errors might be reduced by using an automated method of blood sampling to obtain a more nearly continuous curve, as has been done in animal experiments (*7*).

Errors in measurement of tissue activity were found to result in approximately equivalent errors in rCBF. Thus, improvements in PET scanner accuracy will be directly reflected in the rCBF calculations. Furthermore, the nature of error propagation with the autoradiographic method is more acceptable than with the equilibrium inhalation method using O-15 carbon dioxide, which is also currently in use to measure rCBF with PET (*16,17*). In the latter method, because of a very nonlinear relationship between regional flow and tissue activity, errors in activity measurement are amplified in the calculation of rCBF, and this error propagation changes with local flow rates (*18*). These problems do not occur with the PET autoradiographic method.

This simulation study did not address the issue of the limitation of water as a freely diffusible tracer (*19*). It has been proposed to modify the operational equation of the tissue autoradiographic method by inclusion of the factor $m = 1 - \exp(-PS/f)$, where PS is the product of capillary permeability and surface area (*9*). However, when Eckman et al. (*20*) calculated the value of m in a simulation study, they found it was in fact not a constant, but merely approached the value of $1 - \exp(-PS/f)$ asymptotically with time. Therefore, an appropriate modification of the tissue autoradiographic method to account for diffusion limitation of the tracer is lacking, and this complex issue was not included in our extension of the method to PET. We have chosen to study this problem experimentally by comparing blood flow measured with O-15-labeled water in our PET autoradiographic method to blood flow measured with the intracarotid injection of $H_2{}^{15}O$. The details of these experiments in baboons are reported in the subsequent paper in this series (*4*).

In conclusion, this study of the adaptation of the Kety autoradiographic method shows that it is well suited for the measurement of rCBF in man with PET. An appreciation of the validity of assumptions in the model and of its accuracy will lead to more precise quantification of regional cerebral blood flow with positron emission tomography.

ACKNOWLEDGMENTS

This research was supported by NIH grants NS06833, HL13851, NS14834, RR00396, and RR01380 and the McDonnell Center for Studies of Higher Brain Function. Dr. Herscovitch was a fellow of the Medical Research Council of Canada.

REFERENCES

1. Landau WM, Freygang WH Jr, Rowland LP, et al: The local circulation of the living brain; values in the uanesthetized and anesthetized cat. *Trans Am Neurol Assoc* 80:125–129, 1955
2. Kety SS: Measurement of local blood flow by the exchange of an inert, diffusible substance. *Meth Med Res* 8:228–236, 1960
3. Raichle ME: Quantitative in vivo autoradiography with positron emission tomography. *Brain Res Rev* 1:47–68, 1979
4. Raichle ME, Martin WRW, Herscovitch P: Brain blood flow measured with intravenous $H_2{}^{15}O$. II. Implementation and validation. *J Nucl Med* 24:790–798, 1983
5. Kety SS: The theory and applications of the exchange of inert gas at the lungs and tissues. *Pharmacol Rev* 3:1–41,1951
6. Sakurada O, Kennedy C, Jehle J, et al: Measurement of local cerebral blood flow with iodo[^{14}C]antipyrine. *Am J Physiol* 234.H59–H66, 1978
7. Reivich M, Jehle J, Sokoloff L, et al: Measurement of regional cerebral blood flow with antipyrine-^{14}C in awake cats. *J Appl Physiol* 27:296–300, 1969
8. Eklof B, Lassen NA, Nilsson L, et al: Regional cerebral blood flow in the rat measured by the tissue sampling technique; a critical evaluation using four indicators C^{14}-antipyrine, C^{14}-ethanol, H^3-water and xenon^{133}. *Acta Physiol Scand* 91:1–10, 1974
9. Ginsberg MD: Autoradiographic measurement of cerebral blood flow. In *Cerebral Metabolism and Neural Function.* Baltimore, Williams and Wilkins, 1980, pp 161–169
10. Meyer MW, Werth LJ: Error analysis of a convolution integral approach to estimate local blood flow. *J Appl Physiol* 35:631–634, 1973
11. Mazziotta JC, Phelps ME, Plummer D, et al: Quantitation in positron emission computed tomography: 5. Physical-anatomical effects. *J Comput Assist Tomogr* 5:734–743, 1981
12. Ter-Pogossian MM, Ficke DC, HOOD JT Jr, et al: PETT VI: A positron emission tomograph utilizing cesium fluoride scintillation detectors. *J Comput Assist Tomogr* 6: 125–133. 1982
13. Hoffman EJ, Phelps ME, Huang SC, et al: A new tomograph for quantitative positron emission computed tomography of the brain. *IEEE Trans Nucl Sci* NS-28:99–103, 1981
14. Ter-Pogossian MM, Eichling JO, Davis DO, et al: The determination of regional cerebral blood flow by means of water labeled with radioactive oxygen 15. *Radiology* 93: 31–40, 1969
15. Ginsberg MD, Lockwood AH, Busto R, et al: A simplified in vivo autoradiographic strategy for the determination of regional cerebral blood flow by positron emission tomography: theoretical considerations and validation studies in the rat. *J Cereb Blood Flow Metabol* 2:89–98, 1982
16. Subramanyam R, Alpert NM, Hoop B Jr, et al: A model for regional cerebral oxygen distribution during continuous inhalation of $^{15}O_2$, $C^{15}O$, and $C^{15}O_2$. *J Nucl Med* 19:48–53, 1978
17. Frackowiak RSJ, Lenzi G-L, Jones T, et al: Quantitative measurement of regional cerebral blood flow and oxygen metabolism in man using ^{15}O and positron emission tomography: theory, procedure, and normal values. *J Comput Assist Tomogr* 4:727–736, 1980
18. Jones SC, Greenberg JH, Reivich M: Error analysis for the determination of cerebral blood flow with the continuous inhalation of ^{15}O-labeled carbon dioxide and positron emission tomography. *J Comput Assist Tomogr* 6:116–124, 1982
19. Eichling JO, Raichle ME, Grubb RL Jr, et al: Evidence of the limitations of water as a freely diffusible tracer in brain of the Rhesus monkey. *Circ Res* 35:358–364, 1974
20. Eckman WW, Phair RD, Fenstermacher JD, et al: Permeability limitation in estimation of local brain blood flow with [^{14}C]antipyrine. *Am J Physiol* 229:215–221, 1975

Brain Blood Flow Measured with Intravenous $H_2{}^{15}O$. II. Implementation and Validation

M. E. Raichle, W. R. W. Martin, P. Herscovitch, M. A. Mintun, and J. Markham

Washington University School of Medicine, St. Louis, Missouri

We have adapted the well-known tissue autoradiographic technique for the measurement of regional cerebral blood flow (CBF), originally proposed by Kety and his colleagues, for the measurement of CBF in human subjects using positron emission tomography (PET) and intravenously administered oxygen-15-labeled water. This report describes the steps necessary for the implementation of this PET/autoradiographic technique. In order to establish the accuracy of the method, we measured CBF with intravenously administered oxygen-15-labeled water and PET in anesthetized adult baboons and compared the results with blood flow measured by a standard tracer technique that uses residue detection of a bolus of oxygen-15-labeled water injected into the internal carotid artery. The correlation between CBF measured with PET and the true CBF for the same cerebral hemisphere was excellent. Over a blood-flow range of 10–63 ml/(min · 100 g), CBF (PET) = 0.90 CBF(true) + 0.40 ($n = 23$, $r = 0.96$, $p < 0.001$). When blood flow exceeds 65 ml/(min · 100 g) CBF was progressively underestimated due to the known limitation of brain permeability to water.

J Nucl Med 1983; 24:790–798
DOI: 10.2967/jnumed.252130b

In 1951, Kety presented a theory of inert-gas exchange at the lungs and tissues and its possible application to the measurement of tissue blood flow (*1*). A short time later he and his colleagues described in detail (*2,3*) a tissue autoradiographic technique for the measurement of local brain blood flow in laboratory animals based on this theory of inert-gas exchange. This autoradiographic technique involved the intravenous infusion of radiolabeled trifluoroiodomethane. At the end of 1 min the animal was killed and the brain was removed and sliced in the desired plane for quantitative autoradiography. These quantitative autoradiograms and the time-activity curve of the blood radioactivity formed the basis for the computation of local brain blood flow using Kety's equations (*1*). This technique has been widely applied and revised on several occasions (*4,5*) as newer radiotracers were substituted for the volatile and difficult-to-handle trifluoroiodomethane.

Because positron emission tomography (PET) provides a quantitative measure of local tissue radioactivity and, hence, an in vivo autoradiogram (*6*), we reasoned that local cerebral blood flow could be measured in human subjects using the principles of the Kety autoradiographic technique in conjunction with PET and a freely diffusible, inert pharmaceutical labeled with a positron emitter. In Part I (*7*) we described the theoretical basis for our adaptation of the Kety approach for PET and considered the impact of several potential errors. In this paper we describe the implementation of this technique using $H_2{}^{15}O$ as the diffusible tracer, and present direct experimental evidence concerning its accuracy.

A preliminary report of this work has been presented (*8*).

Received Dec. 21, 1983; revision accepted Apr. 28, 1983.
For reprints contact: M. E. Raichle, MD, Box 8131, Washington University School of Medicine, St. Louis, MO 63110.

METHODS

Animal preparation. CBF was measured in six adult baboons *(Papio papio)* weighing 18 to 25 kg. To facilitate the injection of small aliquots (approximately 0.2 ml) of the baboon's blood labeled with oxygen-15-water into the internal carotid artery, the baboons were anesthetized with phencyclidine (2 mg/kg) at least 2 wk before experiment proper, and the right external carotid artery was ligated at its origin from the common carotid. At the later experiment the radiotracer was injected into the common carotid artery through a small catheter (0.021 cm diam) positioned there under fluoroscopic control.

For the actual comparison of the PET autoradiographic method (*7*) with the standard residue detection technique using the intracarotid administration of oxygen-15-labeled water (*9*) the baboons were anesthetized with ketamine (2 mg/kg), paralyzed with gallamine, intubated with a cuffed endotracheal tube, and passively ventilated on a gas mixture containing 70% nitrous oxide and 30% oxygen. The baboons were then positioned on a special couch that permitted placement of the head in the imaging device or over a 3 in. × 2 in. NaI(Tl) scintillation detector appropriately collimated and positioned under the animal's head so as to ensure essentially uniform detection of a single cerebral hemisphere.

To permit the intracarotid injection of oxygen-15- labeled water, a small catheter was inserted percutaneously into the femoral artery and its tip positioned in the right common carotid artery under fluoroscopic control. To prevent clotting in this arterial catheter system, which was used for the injection of the labeled water, monitoring of blood pressure, and sampling of arterial blood, all animals were heparinized at the beginning of the experiment. Arterial pH, P_{CO2}, and P_{O2} were measured before and after each injection of tracer. To permit the intravenous injection of oxygen-15-labeled water, a small venous catheter was placed percutaneously in the femoral vein.

Positron emission tomography was performed with the PETT VI system (*10*), the design and performance characteristics of which have been discussed elsewhere (*11,12*). Data are recorded simultaneously from seven slices with a center-to-center separation of 14.4 mm. All studies were done in the low-resolution mode, giving an in-plane (i.e., transverse) resolution of 11.7 mm full width at half maximum (FWHM) in the center of the field of view and a slice thickness of 13.9 mm FWHM at the center of the image.

The head of the baboon was positioned with the aid of a vertical laser line such that the center of the lowest slice corresponded to a line running through the center of the cerebral hemispheres. A lateral skull radiograph with this line marked by a vertical radio-opaque wire

provided a permanent record of the position of the lowest PET slice. Because of the size of the adult baboon brain (approximately 150 cc) only data from this bottom slice were used in these experiments. Attenuation correction was uniquely determined for each animal by obtaining a transmission scan using a ring source of activity (germanium-68) fitted to the tomograph as previously described (*10*).

Single-probe data collection

The signal from the single NaI(Tl) scintillation detector produced by the intracarotid injection of $H_2{}^{15}O$ was processed by a pulse- height discriminator with a 60-keV energy window symmetrically bracketing the annihilation peak to minimize scattered radiation. The accepted events (counts) from this single detector were stored in a small laboratory computer. Processing of these data was performed in the computer, including corrections of the count rate for deadtime losses, physical decay of O-15 ($T^1/_2$ = 123 sec), and background, and conversion to a time-activity plotout. Optimal temporal resolution was achieved in the initial portion of the recording by using sampling integration times of 0.1 sec. Statistically smooth recordings were ensured by injection of sufficient activity into the carotid artery to achieve peak counting rates from 10,000 to 20,000 cps.

PET data collection

For the measurement of CBF with PET a 40-sec emission scan (whose modification to permit longer scan times is discussed below) was performed following an intravenous, bolus injection of 5 ml of saline containing 20–30 mCi of oxygen-15-labeled water. Data collections by PET were started at the time of arrival of radioactivity in the brain as judged by a sudden increase in the bank pair coincidence counting rate of the PETT VI system. This was usually 10–15 sec after tracer injection. Zero time for the study was always the actual time tracer administration commenced. The preparation of the radiowater has been described elsewhere (*13*). Arterial blood samples were drawn about every 5 sec from the indwelling carotid catheter, starting at the onset of injection and continuing throughout the scan. These samples were weighed and counted in a well counter to obtain O-15 activity as cps/g blood, corrected for physical decay from the time of injection to the time of measurement. The time-activity curve was then constructed.

Calibration of the tomograph to obtain the regional O-15 concentration in the brain from the reconstructed image (cps/cc tissue) was performed by imaging a phantom divided into six wedge-shaped chambers of equal size. The chambers were filled with varying concentrations of carbon-11-labeled bicarbonate. Aliquots from each chamber were counted in the same well counter used for the measurement of blood radioactivity, and the observed counting rate decay-corrected to the start of the phantom scan. From these data ($Q_{initial}$, in cps/cc), the total counts presented to the scanner by 1 cc of target during the length of the scan (C_{total}, in counts/cc) were obtained by integrating the decay curve over the length of the scan T_S:

$$C_{total} = \int_0^{T_S} C_{initial} \exp(-kt)dt, \tag{1}$$

where k is the decay constant (per sec) for the tracer. After the phantom image was reconstructed, a regression equation was obtained comparing the relative scan data and the directly measured activity in the phantom. From this relationship, the actual local O-15 concentrations can be obtained from each scan.

Because our scanner does not correct for radioactive decay during the data collection, it is necessary to correct scan data for tracer decay that occurs during the study. Our method is derived by assuming a function of activity that would be constant were it not for decay. This is equivalent to computing the average decay over the scan interval T_S, i.e.,

$$\text{average decay} = \int_0^{T_S} \exp(-kT_S)dtbig/T_S \tag{2}$$

$$= \frac{1 - \exp(-kT_S)}{kT_S} \tag{3}$$

Inversion of the average decay yields an "average" decay correction. Simulation studies (unpublished) of various functions equivalent to time-varying head-activity curves likely to be encountered during our studies demonstrate that this method of decay correction is quite adequate (i.e., maximum error <4%).

Data analysis

Single detector system. The time- activity curve obtained subsequent to the intracarotid injection of an aliquot of oxygen-15-labeled water was used to compute the mean cerebral transit time for labeled water ($\bar{t}H_2o$) (*9*). The calculation of CBF from $\bar{t}H_2o$—which we will call CBF(true) to distinguish it from CBF(PET), the CBF deduced from a PET study—is based on the well-established central volume principle of tracer kinetics (*14,15*).

The fraction of oxygen-15-labeled water extracted by the brain during a single capillary transit (E) was determined from the same residue curve used for the measurement of CBF(true) following intracarotid injection of $H_2{}^{15}O$. This single-injection, external-registration technique uses the first 30 sec of the residue curve after the intracarotid injection of labeled water, a method developed in our laboratory for use in vivo with cyclotron-produced positron emitters (*9,16,17*). With this method E is obtained by graphically extrapolating the relatively slow clearance of the labeled water from brain tissue back to the maximum of the perfusion peak, and computing the ratio

$$E = B/A \tag{4}$$

as shown in Fig. 1. As developed in detail elsewhere by ourselves (*17*) and others (*18–20*) the quantity *E* can be related to the tissue blood flow f[ml/(sec. g)], the capillary surface area (S[cm^2/g]) and its permeability (P(cm/sec]) in the following manner:

$$E = 1 - \exp(-PS/f) \tag{5}$$

PET system. The blood curve and scan data were analyzed according to the general principles of inert-gas exchange developed by Kety (*1*) and later embodied in the tissue autoradiographic technique for the measurement of local brain blood flow in laboratory animals (*2–5*). With this method the local blood flow is obtained by numerically solving the following equation for the constant K

$$\begin{aligned} C_i(T) &= \lambda K \int_O^T C_a(t) \exp[-K(T-t)]dt \\ &= \lambda K C_a(T)^* \exp(-KT) \end{aligned} \tag{6}$$

where $C_i(T)$ is the instantaneous local radiotracer concentration (cps/g) at time, T, derived from a quantitative autoradiogram of a brain slice, and $C_a(t)$ is the measured concentration of radiotracer in arterial blood as a function of time, [cps/ml]; and λ is the brain-to-blood equilibrium partition coefficient for the tracer [ml/g]. λ equals 0.95 in our experiment (*9*). The operation of convolution is denoted by the asterisk. The constant K is defined by (*3*):

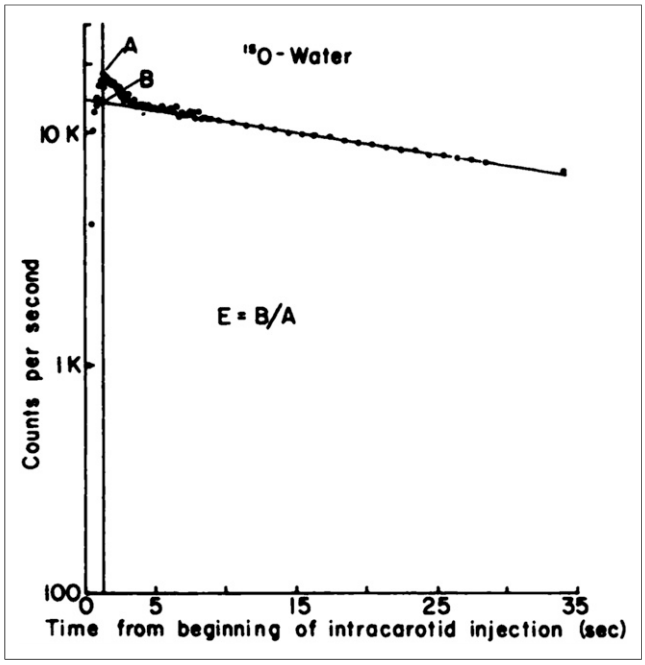

FIGURE 1. Brain time-activity curve (semilog) resulting from intracarotid injection of $H_2{}^{15}O$ in adult baboon. Graphic extrapolation of relatively slow clearance of labeled tissue water back to maximum of perfusion peak allows calculation of fraction of labeled water extracted by tissue (E) during single capillary transit (E = B/A). Application of central volume principle of tracer kinetics (see text) to these data allows computation of cerebral blood flow (CBF), which we designate here as CBF(true). Data in this figure were obtained at cerebral blood flow of 102 ml/(min·100 g).

$$K = mf/\lambda \tag{7}$$

where m is a constant between 0 and 1 that represents the extent to which diffusion Equilibrium between blood and tissue is achieved during passage from the arterial to the venous end of the capillary. As further defined by Kety (*3*)

$$m = 1 - \exp(-PS/f) \tag{8}$$

Thus, m is equivalent to E [Eqs. (7), (8)], a fact that will become important in the analysis of the PET/autoradiographic data (see below).

PET scanners, including the one used in this study (*10*) do not have adequate temporal resolution to measure tissue radioactivity, $C_i(T)$, instantaneously. Thus, to apply the autoradiographic technique to in vivo studies with PET, a scan must run for many seconds, essentially summing the instantaneous radioactivity over time. We have therefore modified the operational equation for this model by an additional integration over the time of the scan (i.e., $T_2 - T_1$) as follows:

$$C = \int_{T_1}^{T_2} C_i(T)dT = \lambda\kappa \int_{T_1}^{T_2} C_a(T)^* \exp(-KT)dT \tag{9}$$

Here, C is the local number of counts per unit weight of tissue recorded by the tomograph from a region of brain tissue during the scan. The time, T_1, is chosen as the time at which there is an appreciable increase above background in a selected bank-pair coincidence counting rate of the PETT VI scanner, thus signifying the arrival of radioactivity of the head. In practice, the constant m is assumed to be 1 in the solution of both the tissue [Eq. (6)] and PET [Eq. (9)] operational equations for K. Thus, from Eq. (7), the flow, f, is equal to λK.

This model relates regional CBF to regional tissue counts and the arterial blood radioactivity curve. Unfortunately, the operational Eq. (9) cannot be solved explicitly for blood flow. It can be solved numerically, however, by means of an interactive parameter estimation technique, although this approach requires significant computing time and would be unwieldy given the large number of spatial data to be analyzed. An alternative approach is to use the operational Eq. (9) to generate a lookup table that relates tissue counts to flow for closely spaced values of flow. This involves numerous evaluations of the equation and would require storage and repetitive searching of the table. Instead, we have expressed the operational equation relating blood flow to tissue counts in terms of a second-order polynomial equation:

$$\text{flow} = A\,(\text{counts})^2 + B\,(\text{counts}).$$

With this function, a parabola going through the origin, the relationship between flow and counts can be fitted with a less than 0.8% inaccuracy in flow for any given number of counts. In comparison, a first-order linear approximation would introduce errors of up to 5% because the operational equation does deviate somewhat from true linearity (see Fig. 2, Ref. 7). The addition of a second-order polynomial term into the fit thus provides greater accuracy.

CBF was calculated for a single, computer-generated region of interest in the center of the baboon brain. This region of interest was a square with 18 pixels on a side. Because each pixel in the tomographic system is 0.27 cm by 0.27 cm in the horizontal plane and approximately 1.4 cm thick, the volume of brain sampled was ~33 cm^3 or, assuming an average brain density of 1.05 g/cc, 34.7 g. Because the adult baboon brain weighs about 150 g, the volume of tissue we sampled for our data is well below a value that might be in error because of partial-volume effects due to sampling of noncerebral tissue. Placing our region of interest centrally, with equal weight given to both cerebral hemispheres, seemed appropriate despite the fact that our CBF(true) was measured only on the right cerebral hemisphere because no significant asymmetries between hemispheres were noted in our data.

Experimental procedure

CBF was varied in the baboons in two ways. First, the arterial carbon dioxide tension was varied by altering the respiratory rate. At least 20 min were allowed between changes in the respiratory rate to permit a new steady state to be achieved. Measurements of arterial blood gases were obtained before and after all measurements of CBF. In addition to varying the arterial CO2 tension we used continuous infusions of sodium pentothal (2 g in 500 ml saline) to achieve blood flows less than 20 ml/(min·100 g).

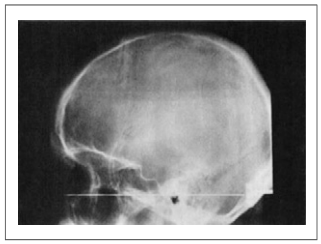

FIGURE 2. Lateral skull radiograph of normal, adult human subject showing position (horizontal, radio-opaque line) of lowest of seven PET slices depicted in Fig. 5. Slices are separated by 14 mm (center to center). Radio-opaque wire is 1 mm in diameter.

In order to evaluate the effect of PET scan length on the accuracy of the PET/autoradiographic technique we used the list-mode data-gathering capabilities of the system (*10*), which permitted us to collect data over a period of 120 sec and then reconstruct them into scans of 0–40 sec, 0–80 sec, or 0–120 sec.

Human studies

A single normal adult study* is presented to illustrate the

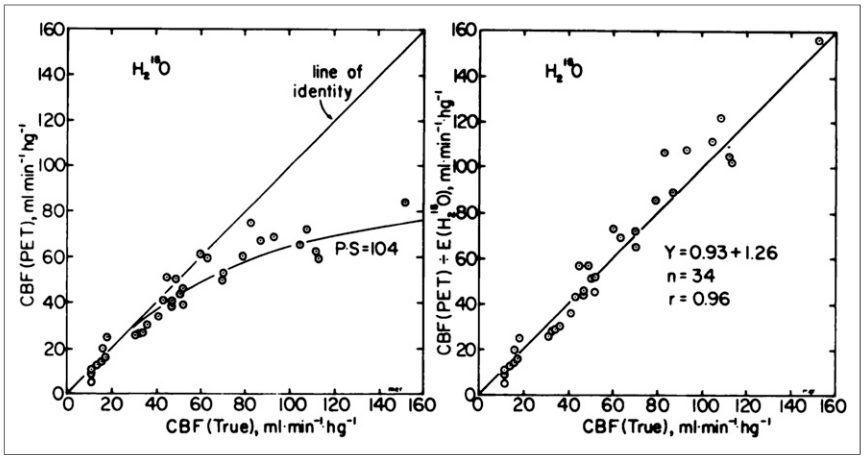

FIGURE 3. Comparison between (a) cerebral blood flow measured in adult baboons using PET/autoradiographic technique [CBF(PET)] with intravenous, bolus injection of $H_2{}^{15}O$, and (b) cerebral blood flow measured in same animal using intracarotid injection of $H_2{}^{15}O$ and residue detection [CBF(true)]. Data on left represent experimental data. In addition to line of identity, figure contains theoretical line based on computed product of brain permeabilty times surface area (P·S) for water for these experiments, 104 ml/(min·100 g). This theoretical line is product of CBF(true) and E estimated from Eq. (8) using CBF(true) as F in Eq. (8) along with measured P·S. For tracer with P·S = 104 ml/(min·100 g), CBF(PET) progressively underestimates CBF(true) when latter exceeds 50 ml/(min·100 g). CBF(PET) data on right have been corrected for measured extraction of $H_2{}^{15}O$ (see text for details).

performance of the PET/autoradiographic technique for the measurement of CBF. The subject was prepared for the study by the percutaneous insertion of a small radial-artery catheter under local anesthesia to permit frequent sampling of arterial blood, and the insertion of an intravenous catheter for tracer injection in the opposite arm. The subject's head was positioned in the same manner as that described, above, for the baboons, including alignment with a vertical laser so that the lowest PET slice corresponded to the subject's orbito-meatal line. A lateral skull radiograph (Fig. 2) was obtained with this line marked by a vertical radio-opaque wire to record permanently the orientation of the PET slices in relation to the bony landmarks of the skull. A molded plastic face mask prevented significant head movement during the PET scan. This system, described in detail elsewhere (*10*), enables accurate repositioning of a subject undergoing sequential studies on different days. After the subject's head was in place in the tomograph, a transmission scan for attenuation correction was performed with a ring phantom containing germanium-68. During the actual measurement of CBF, the room lights were dimmed and the subject instructed to close his eyes. His ears were not plugged. Ambient noise consisted almost entirely of cooling fans from the electronic equipment in the room.

Because blood samples are drawn from the radial artery in most human subjects (our study follows arteriography, in which case the femoral artery is used) to construct the arterial blood time-activity data for Eq. (10), we anticipated that the intravenously injected radioactivity would arrive at our peripheral sampling site at a time that was different from its arrival time in the brain (usually it arrives later at the peripheral site because of the greater distance from the heart). Because the accuracy of our PET/autoradiographic technique is very sensitive to such differences (7) we correct for them in our human studies by determining the arrival time in the head of the subject by observing and recording the time of an abrupt increase in the coincidence counting rate (sampling from a single bank pair (10) once every second) and the arrival time at the peripheral sampling site from the arterial-blood time- activity curve (see Fig. 5). Differences in the recorded delays are reconciled by shifting the arterial time-activity curve by the amount of the difference measured in seconds.

RESULTS

Figure 1 presents the first 30 sec of a typical time- activity curve recorded by our single NaI(Tl) scintillation detector collimated to view the injected right cerebral hemisphere of an adult baboon. From the initial portion of this time-activity curve the cerebral hemisphere extraction (E) of oxygen-15-labeled water is calculated according to Eq. (10) and the procedure depicted in the figure. These same data were used to compute CBF(true), the true cerebral blood flow, according to Eq. (6).

The relationship, based on 36 paired measurements, between the CBF(true) and the CBF(PET) is shown in Fig. 3 (left). Between a CBF of 10 and 60 ml/m(min · 100 g) the relationship between the two measurements is excellent ($Y = 0.90x + 0.40$; $r = 0.96$), but above a CBF of 60 ml/(min·100 g) the CBF(PET) technique progressively underestimates the CBF(true). Because the intracarotid, residue-detection technique allows us to compute not only the CBF(true) but also the extraction (E) of labeled water [Eq. (4); Fig. 1] for each measurement of CBF(PET) we can evaluate the effect of this diffusion limitation

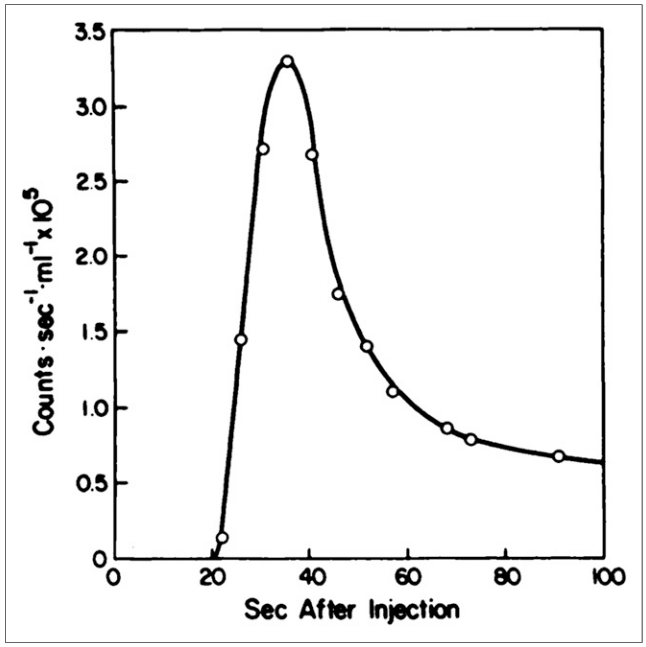

FIGURE 4. Typical human arterial-blood, time-activity curve obtained from radial artery following bolus injection of $H_2{}^{15}O$ in 6 ml of saline into antecubital vein. Note delay in appearance of radioactivity in radial-artery blood (activty injected at time = 0). This delay is compared with delay in arrival of activity in subject's head as signified by abrupt increase in coincidence counts from PETT VI scanner. When differences are observed (radial-artery delay usually exceeds head delay by several seconds) blood curve is shifted to correspond to head delay.

of water on our PET measurement of CBF by dividing each CBF(PET) value by the corresponding value for E. In effect, this corrects for the fact that the value of m [Eq. (9)] is less than the assumed value of 1. The result of this manipulation of the CBF(PET) is shown in Fig. 3 (right). With this correction there occurs excellent agreement between CBF(true) and CBF(PET) over a blood-flow range of 10–155 ml/(minl·100 g). Corresponding to this observation is the fact that there is excellent agreement between the data in Fig. 3 (left) and a line predicted on the basis of the measured P·S for these experiments in the adult baboon [P·S = 104 ± 11.2 (s.d.); n = 25]. This theoretical line is simply the product of CBF(true) and E estimated from Eq. (8), using CBF(true) as F in Eq. (8) along with the measured P·S for these experiments. Note that P·S could be computed on only 25 of the 36 experiments, because at low CBF where E is unity, P·S is indeterminate.

Varying the length of data collection by PET on the CBF computed by the PET/autoradiographic technique—from the usual 40 sec (i.e., all data in Fig. 2) to 80 or 120 sec—leads to estimates of CBF that decrease as a function of the acquisition time. Thus, in a typical case of CBF decreased from 38 ml/(min·100 g) as measured with the usual 40-sec scan to 32 ml/(min·100 g) with an 80-sec scan and 27 ml/(min·100 g) with a 120-sec scan. A similar decline was observed when the scan length was maintained at 40 sec but the starting time following injection was progressively delayed.

Data from a single, normal, young adult male are shown in Figs. 4 and 5. Typical intravenous injections of 60 to 80 mCi of $H_2{}^{15}O$ result in bank pair coincidence count rates of 30,000 to 45,000 cps with the PETT VI tomograph in adult subjects. Figure 4 shows the blood time-activity (corrected for decay of 015) resulting from the intravenous (antecubital) bolus injection of 82 mCi of oxygen-15-labeled water in 6 ml of normal saline. Figure 5 shows data obtained from this study (scan duration = 40 sec).

DISCUSSION

To the best of our knowledge, these data represent the first direct comparison of the classic Kety tissue autotechnique (*1–3*) with another established technique (i.e., the central volume principle; *14,15*) for the measurement of CBF with diffusible, inert indicators. The choice of the latter technique as our standard for comparison seemed especially appropriate to us because it is not affected by the known permeability limitation of the brain for water (*9,15*). Thus, failure of the PET/autoradiographic technique to estimate accurately the true CBF as the result of a tracer that does not diffuse freely between blood and brain tissue should be easily detectable and quantifiable.

Our data (Fig. 3) clearly indicate that a brain permeability limitation for $H_2{}^{15}O$ causes an underestimation of CBF, using the PET/autoradiographic technique, when the true brain blood flow exceeds about 60 ml/(min·100 g) in the adult baboon. Values for CBF(PET) above this flow rate are predictably scaled by the extraction of $H_2{}^{15}O$ [i.e., E, Eq. (4), or m, Eq. (10)] for that blood flow. Three observations support this interpretation of our data. First, division of the CBF(PET) value for blood flow by the extraction of $H_2{}^{15}O$ for each experiment, measured by the intracarotid injection of $H_2{}^{15}O$ [Eq. (4); Fig. 1], produces a linear relationship between CBF(true) and CBF(PET) over the entire

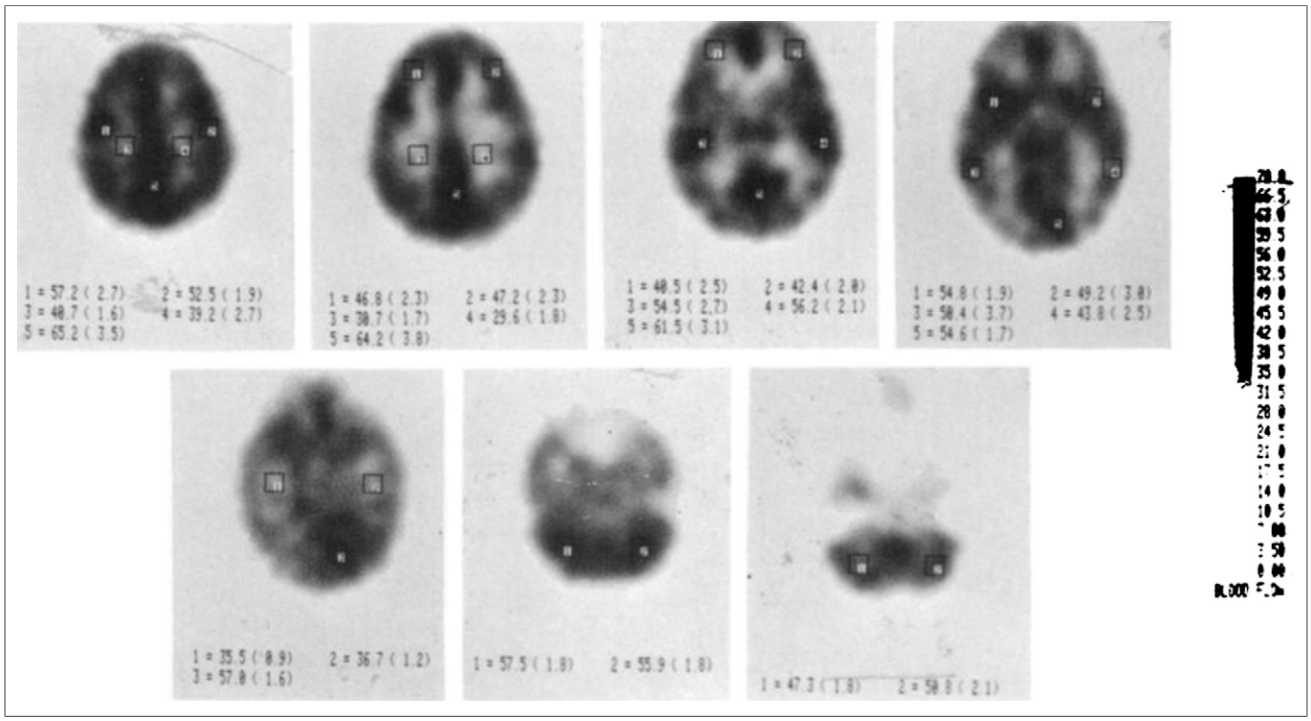

FIGURE 5. Typical quantitative meastrement of local cerebral blood flow (CBF) in normal, adult, male subject using intravenous bolus injection of 82 mCi of $H_2{}^{15}O$ and adaptation (*7*) of classic Kety tissue autoradiographic technique (*3*). Data were collected over 40 sec.The quantitative gray scale [ml/(min·100g)] was set to same maximum [i.e., 70 ml/(min·100 g)] for each slice to permit more accurate visual comparison. Specific regions have been selected in each slice (i.e., numbered boxes) to illustrate local variations in blood flow. Values for these regions are listed just below each slice along with standard deviation of 25 pixels in each region.

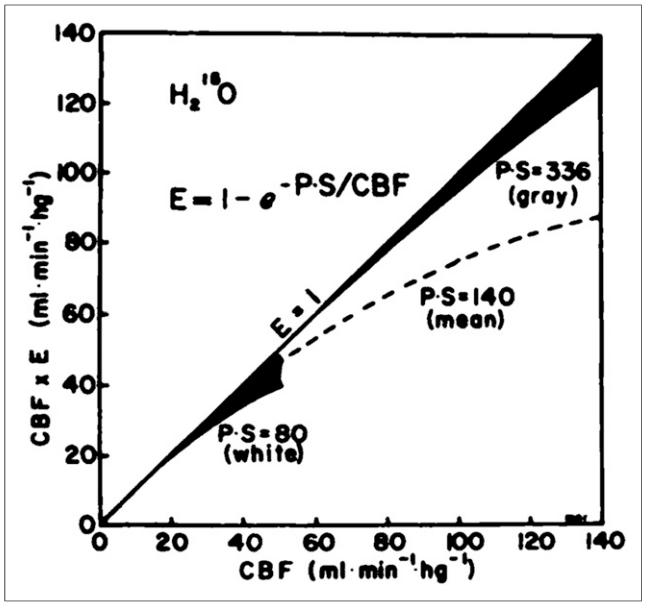

FIGURE. 6. Hypothetical relationship between cerebral blood flow (CBF) measured with PET/autoradiographic technique in humans (y-axis) and true CBF (x-axis) assuming product of brain white-matter permeability times surface area (P·S) for $H_2{}^{15}O$ of 80 ml/(min·100 g) and brain gray matter P S for $H_2{}^{15}O$ of 336 ml/(min·100 g). These values for P·S of $H_2{}^{15}O$ are based on whole-brain average for human of 140 ml/(min·100 g) (*24*). Errors predicted on basis of this analysis are shown as stippled deviations from line of identity.

range of blood flow examined (Fig. 3, right). This manipulation of the experimental data is equivalent to specifying a unique value for m [Eq. (7)], which is normally assumed to have a value of 1 (*2,3*). Second, the average value for the product (P·S) of brain permeability and surface area, estimated from our data [Eq. (8)] allows us to predict the relationship between the blood flow measured by the PET/autoradiographic technique and the CBF(true). We have illustrated this in Fig. 3 (left) where we have plotted the product of f [i.e., true blood flow per unit weight of tissue, Eq. (6)] and m [Eq. (8)] as a function of CBF(true). It can readily be seen that with a tracer whose apparent P·S product is 104 ml/(min·100 g), CBF is progressively underestimated when blood flow exceeds a value of about 40 ml/(min·100 g). It is also apparent that our experimental data correspond quite well to this hypothetical relationship. Finally, studies of the PET/ autoradiographic model using C-11 butanol as the diffusible, inert tracer (to be published separately) demonstrate a linear relationship (i.e., line of identity) between CBF(PET) and CBF(true) [maximum blood flow 120 ml/(min·100 g)]. Because C-11 butanol freely diffuses across the blood-brain barrier (*16*), this observation further supports our hypothesis that our experimental results reflect the known brain permeability limitation of $H_2{}^{15}O$.

Other investigators have previously noted that the tissue autoradiographic technique is sensitive to the brain permeability of the diffusible tracer chosen (*5,21,22*). These observations led to several changes in the choice of tracer for tissue autoradiographic work in small laboratory animals in which CBF can occasionally reach 200-400 ml/(min·100 g).

It is important to understand the clinical implications of this brain-permeability limitation of $H_2{}^{15}O$ when it is utilized as the diffusible tracer for the PET/autoradiographic technique. Two facts make us optimistic that $H_2{}^{15}O$ will perform quite satisfactorily for studies in humans despite its P·S limitation. Fust, the average brain permeability for water in humans is somewhat higher than we have measured in the baboon in these experiments [i.e., ~104 ml/(min·100 g)]. Paulson and his colleagues report an average P for water in the human brain of 2.4×10^{-4} cm/sec (*23*). Assuming an average human brain, with capillary surface area of 100 cm^2/g (see below), this yields an average P·S (i.e., for gray plus white matter) of 144 ml/(min·100 g) for the human brain. From these data we can estimate that CBF(PET) for the brain as a whole will appreciably underestimate CBF(true) only when the blood flow exceeds ~55 ml/(min·100 g). Second, the above analysis as well as the presentation of our data (Fig. 3) assume a uniform P·S for the brain. Although it is probably reasonable to assume a uniform vascular permeability for the brain, it is not reasonable to assume a uniform capillary surface area when contemplating regional studies in man with PET. In fact, capillary surface area is estimated by others to vary from 190 cm^2/cm^3 in human cerebral cortex to 57 cm^2/cm^3 in human cerebral white matter (*20,24*). Using these data for S one can estimate the true water P·S of gray and white matter from the estimate of human whole-brain P provided by Paulson et al. (i.e., 2.4×10^{-4} cm/sec; Ref. *23*). Such an estimate of water P·S for gray and white matter, and the implication it has for the accuracy of the PET/autoradiographic technique are shown in Fig. 6. Based on this information we are quite confident that the PET/autoradiographic technique will perform accurately when applied to regional studies in human subjects (e.g., see Fig. 5). An important test of this assumption will be a direct region-by-region comparison of local CBF measured sequentially with the PET/autoradiographic technique in the same human subject using $H_2{}^{15}O$ and C-11 butanol. We are currently planning this study.

We emphasize the advantages of $H_2{}^{15}O$ over alternative inert tracers, labeled with longer-lived radionuclides, that might be selected because of their greater blood-brain barrier permeability (e.g., C-11 butanol, C-11 iodoantipyrine). Because the data collection time for the PET/autoradiographic method must be short (i.e., ≤40 sec; see below), approximately equivalent millicurie doses of radiopharmaceutical must be used regardless of the radionuclide. This results in an appreciably higher dose to the subject when longer-lived, positron-emitting radionuclides are used, and more prolonged residual background activity must be tolerated. The consequence of these effects is to reduce greatly the number and frequency of measurements that can be made safely in a single subject. Using $H_2{}^{15}O$, for example, we have made as many as eight sequential measurements of CBF in a single sitting with the measurements spaced about 12 to 15 min apart. Such a protocol, used in our case for functional mapping of the brain, would be difficult, if not impossible, with tracers labeled with N-13, C-11, or F-18.

There is one very important constraint that must be placed on the use of the PET/autoradiographic technique as well as on the classic tissue autoradiographic technique itself (*5*). The duration of the study must not exceed 1 min, as originally prescribed by Kety and others (*2–5*). Data collections in excess of this time period show an underestimation of CBF that increases with time. This phenomenon is also shown in the data of Eklof et al. (*21*). In the latter study the classic autoradiographic technique was used but direct tissue sampling was substituted for the actual tissue autoradiography. Examining several tracers with differing permeabilities (i.e., antipyrine, ethanol, water, and xenon), Eklof et al. (*21*) observed a decline in the measured blood flow as the tissue data collection was delayed from 30 sec to 60 or 120 sec. We do not have an explanation for this

phenomenon. It is quite clearly not related to any aspect of the PET adaptation of the original Kety autoradiographic technique because it occurs in applications of the original technique (*21*) as well as in our work. It is definitely not due to the permeability of a particular tracer. We have observed the phenomenon with C-11 butanol as well as $H_2{}^{15}O$ (unpublished data). Eklof et al. (*21*) have observed it with an additional group of tracers with widely differing permeabilities. It is not due to tissue inhomogeneity, as Eklof et al. (*21*) discuss in detail. Until this problem has been solved, investigators must be cautioned to use this technique—whether in the original form or in the PET adaptation—with strict attention to the length of data collection. This *must not exceed* 1 min for accurate, quantitative results.

One practical feature of the PET/autoradiographic technique should be emphasized. Because the tissue concentration of radionuclide is related to local blood flow in a nearly linear manner (*7*), a PET *image* of the distribution of $H_2{}^{15}O$ or other suitable radiopharmaceutical (e.g., C-11 butanol) is an accurate representation of local tissue blood flow. Where regional comparisons in the same brain provide the desired clinical information, sampling of arterial blood may be unnecessary. In addition, accumulating data in humans (to be published separately) indicate that comparisons between sequential scans in the same person can be made when the scans are scaled to the exact amount of $H_2{}^{15}O$ injected and careful attention is paid to the positioning of the subject in the PET scanner.

Finally, when sampling of arterial blood from a radial artery is necessary for a truly quantitative measurement of CBF using the PET/autoradiographic technique, we stress that this can be accomplished with relative safety and minimal discomfort to the human subject. The risk to the subject is minimized by performing an Allen test (*25*) to document a dual arterial supply to the hand; and using a 20-gauge or smaller Teflon catheter for relatively short periods of time (*26*). At the time of this writing, we have performed approximately 360 such catheterizations without a complication. Our experience agrees with the much greater experience of others that suggests a complication rate (i.e. major ischemic complication) of less than one in 1000 (*27–29*).

FOOTNOTE

*Permission for this study was obtained from the subject in accordance with guidelines approved for this study by the Human Studies Committee of Washington University and the Radioactive Drug Research Committee (Washington University) of the Food and Drug Administration.

ACKNOWLEDGMENT

This research was supported by NIH grants NS06833, NS14834, HL13851, RR00396, and RR01380. Drs. Herscovitch and Martin were Fellows of the Medical Research Council of Canada.

REFERENCES

1. Kety SS: The theory and application of the exchange of inert gas at the lungs and tissues. *Pharmacol Rev* 3:1–41,1951
2. Landau WM, Freygang WH Jr, Rowland LP, et al: The local circulation of the living brain; values in the unanesthetized and anesthetized cat. *Trans Am Neurol Assoc* 80:125–129,1955
3. Kety SS: Measurement of local blood flow by the exchange of an inert, diffusible substance. *Methods Med Res* 8:228–236,1960
4. Reivich M, Jehle J, Sokoloff L, et al: Measurement of regional cerebral blood flow with antipyrine-^{14}C in awake cats. *J Appl Physiol* 27:296–300, 1969
5. Sakurada O, Kennedy C, Jehle J, et al: Measurement of local cerebral blood flow with iodo[^{14}C]antipyrine. *Am J Physiol* 234:H59–H66, 1978
6. RaichLE ME: Quantitative in vivo autoradiography with positron emission tomography. *Brain Res Rev* 1:47–68, 1979
7. Herscovitch P, Markham J, Raichle ME: Brain blood flow measured with intravenous H2^{15}O. I. Theory and error analysis. *J Nucl Med* 24:782–789,1983
8. Herscovitch P, Markham J, Raichle ME: Accuracy of the Kety autoradiographic measurement of cerebral blood flow adapted for positron emission tomography. *J Nucl Med* 23:P13, 1982 (abstr)
9. Eichling JO, Raichle ME, Grubb RL Jr, et al: Evidence of the limitation of water as a freely diffusible tracer in brain of the Rhesus monkey. *Circ Res* 35:358–364, 1971
10. Ter-Pogossian MM, Ficke DC, Hood JT Sr, et al: PETT VI: A positron emission tomograph utilizing cesium fluoride scintillation detectors. *J Comput Assist Tomogr* 6: 125–133, 1982
11. Ficke DC, Beecher DE, Hoffman GR, et al: Engineering aspects of PETT VI. *IEEE Trans Nucl Sci* 29: 474–478, 1982
12. Yamamoto M, Ficke DC, Ter-Pogossian MM: Performance study of PETT VI, a positron computed tomograph with 288 cesium fluoride detectors. *IEEE Trans Nucl Sci* 29:529–533, 1982
13. Welch MJ, Lifton JT, Ter-Pogossian MM: Preparation of millicurie quantities of oxygen-15-labeled water. *J Labelled Compd* 5:168–172,1969
14. Zierler KL: Equations for measuring blood flow by external monitoring of radioisotopes. *Circ Res* 16:309–321, 1965
15. Roberts GW, Larson KB, Spaeth PE: The interpretation of mean transit time measurements for multiphase systems. *J Theor Biol* 39:447–475, 1973
16. Raichle ME, Eichling JO, Straatmann MG, et al: Blood-brain barrier permeability of ^{11}C-labeled alcohols and ^{15}O-labeled water. *Am J Physiol* 230:543–552,1976
17. Raichle ME, Larson KB: The significance of the NH_3-$NH_4{}^+$ equilibrium on the passage of ^{13}N-ammonia from blood to brain. A new regional residue detection model. *Circ Res* 48:913—937, 1981
18. Sangren WC, Sheppard CW: A mathematical derivation of the exchange of a labeled substance between a liquid flowing in a vessel and an external compartment. *Bull Math Biophys* 15:387–394,1953
19. Renkin EM: Transport of potassium-42 from blood to tissue in isolated mammalian skeletal muscles. *Am J Physiol* 197: 1205–1210,1959
20. Crone C: The permeability of capillaries in various organs as determined by use of the "indicator diffusion" method. *Acta Physiol Scand* 58:292–305,1963
21. EklOf B, Lassen NA, Nilsson L, et al: Regional cerebral blood flow in the rat measured by the tissue sampling technique; a critical evaluation using four indicators C^{14}-antipy- rine, C^{14}-ethanol, H^3-water and xenon^{133}. *Acta Physiol Scand* 91:1–10,1974
22. Eckman WW, Phair RD, Fenstermacher JD, et al: Permeability limitation in estimation of local brain blood flow with [^{14}C]antipyrine. *Am J Physiol* 229: 215–221, 1975
23. Paulson OB, Hertz MM, Bolwig TG, et al: Filtration and diffusion of water across the blood-brain barrier in man. *Microvasc Res* 13:113–124, 1977
24. Cobb S: Cerebrospinal blood vessels. In *Penfield's Cytology and Cellular Pathology of the Nervous System.* New York, Hoeber, 1932, Vol II, pp 577–610
25. Oh TE, Davis NJ: Radial artery cannulation. *Anaesth Intens Care* 3:12–18, 1975
26. Davis FM: Radial artery cannulation: influence of catheter size and material on arterial occlusion. *Anaesth Intens Care* 6:49–53, 1978
27. Dalton B, Laver MB: Vasospasm with an indwelling radial artery cannula. *Anesthesiology* 34:194–197,1971
28. Bedford RF, Wollman H: Complications of percutaneous radial-artery cannulation: an objective prospective study in man. *Anesthesiology* 38:228–236, 1973
29. Davis FM, Stewart JM: Radial artery cannulation: a prospective study in patients undergoing cardiothoracic surgery. *Br J Anaesth* 52:41–47,1980